

# $^1\text{H}$ , $^{13}\text{C}$ and $^{15}\text{N}$ NMR spectral analysis of substituted 1,2,3,4-tetrahydro-pyrido [1,2-*a*]pyrimidines

Ulrich Girreser,\* Ullvi Bluhm, Bernd Clement and Dieter Heber



The NMR spectroscopic data of a series of thirty-four 3-acylpyrido[1,2-*a*]pyrimidinium salts are analyzed, which were prepared as either perchlorates or chlorides. Methyl group substituted 3-aryltetrahydropyrido[1,2-*a*]pyrimidines with the methyl substituent in positions 6, 8 and 9 as well as both in positions 6 and 8 were investigated bearing various aryl substituents. Unequivocal assignment of all resonances was achieved via two-dimensional  $^1\text{H}$ ,  $^1\text{H}$ -COSY measurements,  $^1\text{H}$ ,  $^{13}\text{C}$  and  $^1\text{H}$ ,  $^{15}\text{N}$  HSQC as well as HMBC experiments, and important diagnostic CH and NH couplings in the heteroaromatic ring system are evaluated. The influence of the methyl substituents was analyzed on the proton, carbon and nitrogen shifts. A significant effect of the counter ion on some chemical shifts of the nuclei under discussion of the pyridopyrimidines is found, allowing the indirect detection of the anion, which is confirmed by direct measurement of the  $^{35}\text{Cl}$  nucleus of the perchlorates. Copyright © 2013 John Wiley & Sons, Ltd.

Supporting information may be found in the online version of this article.

**Keywords:** structure analysis; pyrido[1,2-*a*]pyrimidines; NMR spectroscopy;  $^1\text{H}$  NMR;  $^{13}\text{C}$  NMR;  $^{15}\text{N}$  NMR;  $^{35}\text{Cl}$  NMR; counter ion effects

## Introduction

Some years ago, we presented a simple synthetic approach to enone Mannich bases **2** via condensation of aromatic ketones **1** with paraformaldehyde (Scheme 1).<sup>[1]</sup> These enone Mannich bases could be condensed with a number of bifunctional nucleophiles<sup>[2]</sup> like amidines<sup>[3]</sup> or aminopyridines<sup>[4]</sup> in order to access the corresponding heterocyclic derivatives such as tetrahydropyrimidines or pyrido[1,2-*a*]pyrimidines, some structures showing promising pharmacological properties.<sup>[5]</sup> Consequently, the approach to pyrido[1,2-*a*]pyrimidines was exploited for the search of new NO synthase inhibitors.<sup>[6]</sup> A great number of structures were made available by using methyl-substituted aminopyridines as precursors to afford pyridopyrimidines with varying aryl substituents in position 3 and methyl groups in positions 6, 8 and 9 (structures **5–8**) and 6,8-position (pyrimidines **8**); additionally, pyridopyrimidines **4** without methyl group were synthesized (Scheme 1). The products were isolated as either hydroperchlorate or hydrochloride salts. They were characterized by their  $^1\text{H}$  NMR spectra, the conventional electron impact mass spectra and elemental analysis, or high resolution mass spectroscopy. Furthermore, the lipophilicity of these structures was determined.<sup>[6]</sup> Some members show a remarkable NOS inhibition; however, the selectivity for the three isoforms (nNOS, iNOS and eNOS) is not in a range to propose further structural development.<sup>[6]</sup>

Continuing our investigations, we considered heteronuclear chemical shifts as an important tool for the analysis of the tetrahydro-pyrido[1,2-*a*]pyrimidines **4–8**, so all structures were investigated using standard NMR pulse techniques to assign, evaluate and compare the homo- and heteronuclear spectra of these compounds. Of special interest was the effect of substitution on the  $^{15}\text{N}$  NMR shifts and the influence of the counter ion, as either hydrochloric acid or perchloric acid was necessary to

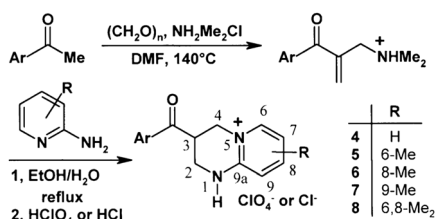
achieve precipitation of the pyridopyrimidines **4–8** during the synthetic protocol. In total, 34 compounds (Fig. 1) were analyzed, and the variability for this data set is generated by (i) varying aryl substituents in position 3, (ii) the position of the methyl group(s), (iii) the different counter ions perchlorate or chloride, (iv) the varying concentrations of the samples (a factor of 2), and (v) the different lipophilicity of the structures in the range of 1.4 to 2.8.<sup>[6]</sup> Only the unsubstituted 1,2,3,4-tetrahydro-pyrido [1,2-*a*]pyrimidinium bromide has been reported with  $^1\text{H}$  and  $^{13}\text{C}$  NMR shifts without assignment.<sup>[7]</sup>

## Experimental

The synthesis and the description of other physical and spectroscopic properties of the 1,2,3,4-tetrahydro-pyrido[1,2-*a*]pyrimidines are described elsewhere.<sup>[3,6]</sup> The following compounds were investigated: 3-benzoyl-1,2,3,4-tetrahydro-2*H*-pyrido[1,2-*a*]pyrimidine hydroperchlorate (**4a**), 1,2,3,4-tetrahydro-3-(4-methylbenzoyl)-2*H*-pyrido[1,2-*a*]pyrimidine hydroperchlorate (**4b**), 3-(4-bromobenzoyl)-1,2,3,4-tetrahydro-2*H*-pyrido[1,2-*a*]pyrimidine hydrochloride (**4c**), 3-(3,4-dichlorobenzoyl)-1,2,3,4-tetrahydro-2*H*-pyrido[1,2-*a*]pyrimidine hydrochloride (**4d**), 1,2,3,4-tetrahydro-3-(3,4-dimethoxybenzoyl)-2*H*-pyrido[1,2-*a*]pyrimidine hydroperchlorate (**4e**), 3-(4-fluorobenzoyl)-1,2,3,4-tetrahydro-2*H*-pyrido[1,2-*a*]pyrimidine hydroperchlorate (**4f**), 1,2,3,4-tetrahydro-3-(3,4,5-trimethoxybenzoyl)-2*H*-pyrido[1,2-*a*]

\* Correspondence to: Ulrich Girreser, Pharmaceutical Institute, Department of Pharmaceutical Chemistry, Christian-Albrechts-University of Kiel, Gutenbergstraße 76, D-24118 Kiel, Germany. E-mail: girreser@pharmazie.uni-kiel.de

Pharmaceutical Institute, Department of Pharmaceutical Chemistry, Christian-Albrechts-University of Kiel, Gutenbergstraße 76, D-24118 Kiel, Germany



**Scheme 1.** Synthesis of substituted 1,2,3,4-tetrahydro-pyrido[1,2-*a*]pyrimidines **4–8**.

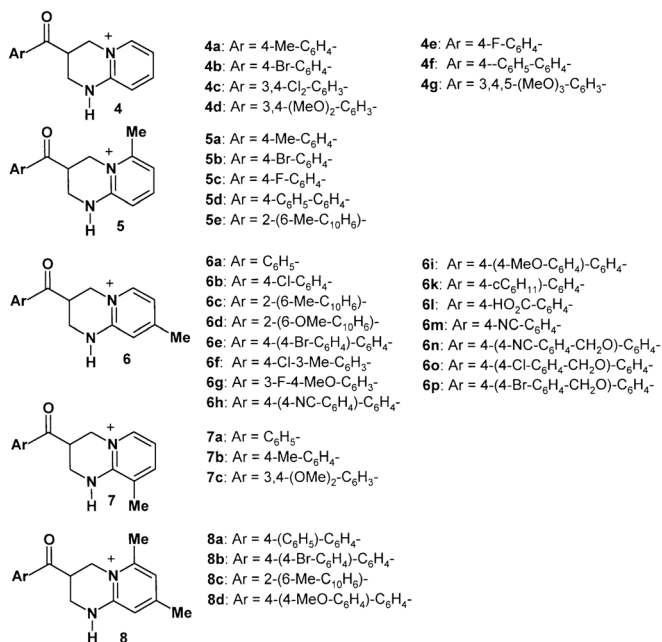


**Figure 1.** Structures of pyridopyrimidines **4–8** investigated.

pyrimidine hydrochloride (**4g**), 1,2,3,4-tetrahydro-6-methyl-3-(4-methylbenzoyl)-2*H*-pyrido[1,2-*a*]pyrimidine hydroperchlorate (**5a**), 1,2,3,4-tetrahydro-3-(3,4-dimethoxybenzoyl)-6-methyl-2*H*-pyrido[1,2-*a*]pyrimidine hydroperchlorate (**5b**), 3-(4-fluorobenzoyl)-1,2,3,4-tetrahydro-6-methyl-2*H*-pyrido[1,2-*a*]pyrimidine hydroperchlorate (**5c**), 1,2,3,4-tetrahydro-6-methyl-3-(4-phenylbenzoyl)-2*H*-pyrido[1,2-*a*]pyrimidine hydrochloride (**5d**), 1,2,3,4-tetrahydro-6-methyl-3-[2-(6-methylnaphthoyl)]-2*H*-pyrido[1,2-*a*]pyrimidine hydroperchlorate (**5e**), 1,2,3,4-tetrahydro-8-methyl-3-benzoyl-2*H*-pyrido[1,2-*a*]pyrimidine hydroperchlorate (**6a**), 3-(4-chlorobenzoyl)-1,2,3,4-tetrahydro-8-methyl-2*H*-pyrido[1,2-*a*]pyrimidine hydroperchlorate (**6b**), 1,2,3,4-tetrahydro-8-methyl-3-[2-(6-methylnaphthoyl)]-2*H*-pyrido[1,2-*a*]pyrimidine hydroperchlorate (**6c**), 1,2,3,4-tetrahydro-[2-(6-methoxynaphthoyl)]-8-methyl-3-2*H*-pyrido[1,2-*a*]pyrimidine hydroperchlorate (**6d**), 3-[4-(4-bromophenyl)benzoyl]-1,2,3,4-tetrahydro-8-methyl-2*H*-pyrido[1,2-*a*]pyrimidine hydroperchlorate (**6e**), 3-(4-chloro-3-methylbenzoyl)-1,2,3,4-tetrahydro-8-methyl-2*H*-pyrido[1,2-*a*]pyrimidine hydroperchlorate (**6f**), 3-(3-fluoro-4-methoxybenzoyl)-1,2,3,4-tetrahydro-8-methyl-2*H*-pyrido[1,2-*a*]pyrimidine hydroperchlorate (**6g**), 3-[4-(4-cyanophenyl)benzoyl]-1,2,3,4-tetrahydro-8-methyl-2*H*-pyrido[1,2-*a*]pyrimidine hydrochloride (**6h**), 1,2,3,4-tetrahydro-3-[4-(4-methoxyphenyl)benzoyl]-8-methyl-2*H*-pyrido[1,2-*a*]pyrimidine hydroperchlorate (**6i**), 3-(4-cyclohexylbenzoyl)-1,2,3,4-tetrahydro-8-methyl-2*H*-pyrido[1,2-*a*]pyrimidine hydroperchlorate (**6k**), 3-(4-carboxylatobenzoyl)-1,2,3,4-tetrahydro-8-methyl-2*H*-pyrido[1,2-*a*]pyrimidine hydrochloride (**6l**),

3-(4-cyanobenzoyl)-1,2,3,4-tetrahydro-8-methyl-2*H*-pyrido[1,2-*a*]pyrimidine hydroperchlorate (**6m**), 3-[4-(4-cyanobenzoyloxy)benzoyl]-1,2,3,4-tetrahydro-8-methyl-2*H*-pyrido[1,2-*a*]pyrimidine hydroperchlorate (**6n**), 3-[4-(4-chlorobenzoyloxy)benzoyl]-1,2,3,4-tetrahydro-8-methyl-2*H*-pyrido[1,2-*a*]pyrimidine hydroperchlorate (**6o**), 3-[4-(4-bromobenzoyloxy)benzoyl]-1,2,3,4-tetrahydro-8-methyl-2*H*-pyrido[1,2-*a*]pyrimidine hydrochloride (**6p**), 3-benzoyl-1,2,3,4-tetrahydro-9-methyl-2*H*-pyrido[1,2-*a*]pyrimidine hydroperchlorate (**7a**), 1,2,3,4-tetrahydro-9-methyl-3-(4-methylbenzoyl)-2*H*-pyrido[1,2-*a*]pyrimidine hydroperchlorate (**7b**), 1,2,3,4-tetrahydro-3-(3,4-dimethoxybenzoyl)-9-methyl-2*H*-pyrido[1,2-*a*]pyrimidine hydroperchlorate (**7c**), 1,2,3,4-tetrahydro-6,8-dimethyl-3-(4-phenylbenzoyl)-2*H*-pyrido[1,2-*a*]pyrimidine hydroperchlorate (**8a**), 3-[4-(4-bromophenyl)benzoyl]-1,2,3,4-tetrahydro-6,8-dimethyl-2*H*-pyrido[1,2-*a*]pyrimidine hydroperchlorate (**8b**), 1,2,3,4-tetrahydro-6,8-dimethyl-3-[2-(6-methylnaphthoyl)]-2*H*-pyrido[1,2-*a*]pyrimidine hydroperchlorate (**8c**) and 1,2,3,4-tetrahydro-6,8-dimethyl-3-[2-(6-methylnaphthoyl)]-2*H*-pyrido[1,2-*a*]pyrimidine hydrochloride (**8d**).

### NMR measurements – general

All spectra were obtained on a Bruker Avance III 300 spectrometer (Bruker, Rheinstetten, Germany) with a variable temperature unit at 300 K calibrated with methanol-*d*<sub>4</sub><sup>[8]</sup> with a multinuclear probe head using the manufacturer's pulse programs described later on. All spectra were recorded in DMSO-*d*<sub>6</sub> as solvent. The compounds are not sufficiently soluble in other solvents like CDCl<sub>3</sub> or D<sub>2</sub>O. Between 8 and 25 mg of the pyridopyrimidinium salt was used in 0.5 ml of solvent. Furthermore, 2 μl of nitromethane were added as a 20% solution in DMSO-*d*<sub>6</sub> as internal standard for the <sup>15</sup>N NMR measurements (30.4 MHz) with <sup>15</sup>N NMR δ = 0.0 ppm, affording an additional signal at 4.46 ppm (<sup>1</sup>H) and 63.5 ppm (<sup>13</sup>C). For the more lipophilic structures, heating of the samples for complete dissolution was necessary. <sup>1</sup>H (300 MHz) and <sup>13</sup>C (75.4 MHz) spectra were referenced to internal DMSO-*d*<sub>5</sub> (<sup>1</sup>H NMR δ 2.50 ppm) and internal DMSO-*d*<sub>6</sub> (<sup>13</sup>C NMR δ 39.5 ppm). For <sup>19</sup>F NMR (282 MHz) measurements, external CFCl<sub>3</sub> in DMSO-*d*<sub>6</sub> was used (<sup>19</sup>F δ 0.0 ppm using the second largest peak); for <sup>35</sup>Cl NMR measurements (29.4 MHz), external NaCl (0.1 M in D<sub>2</sub>O, <sup>35</sup>Cl NMR, δ 0.0 ppm) was used. All coupling constants (*J* values) are quoted in Hz.

### <sup>1</sup>H NMR and <sup>13</sup>C NMR measurements

Conventional one-dimensional proton and proton-decoupled carbon spectra using a 30° flip angle were measured. A gradient-enhanced double-quantum filtered nonphase sensitive <sup>1</sup>H, <sup>1</sup>H COSY spectrum with 512 *t*<sub>1</sub> increments was recorded in order to evaluate the coupling proton and unresolved diagnostic H,H long range couplings. For the recording of <sup>1</sup>H,<sup>13</sup>C correlations, gradient-enhanced HSQC spectra were used with carbon decoupling with 512 *t*<sub>1</sub> increments, an interpulse delay of 1.5 s and two repetitions per *t*<sub>1</sub> increment. For the recording of gradient-enhanced <sup>1</sup>H,<sup>13</sup>C HMBG spectra without <sup>13</sup>C decoupling, the pulse program with two low-pass filters was employed with 256 *t*<sub>1</sub> increments, an interpulse delay of 1.5 s and eight repetitions per *t*<sub>1</sub> increment. Delays were optimized for a coupling constant of 8 Hz. The determination of CH long range coupling constants was achieved via the EXSIDE pulse program with selective excitation using a shaped pulse with a length of 50 ms providing sufficient selectivity in most cases; in a few cases, a length of 120 ms was necessary. 1024 *t*<sub>1</sub> increments, an interpulse delay of 2 s, four or eight repetitions per *t*<sub>1</sub> increment and a *J* factor of 30 were used.

### <sup>15</sup>N NMR measurements

<sup>15</sup>N data are obtained via indirect detection of proton resonances. So, for the recording of <sup>1</sup>H,<sup>15</sup>N gradient-enhanced HSQC spectra, a sweep width of 550 ppm, 1024 *t*<sub>1</sub> increments, an acquisition time of 0.24 s, an interpulse delay of 1.5 s and two repetitions per *t*<sub>1</sub> increment were employed. Resolution enhancement was achieved via linear prediction. The calibration of this <sup>1</sup>H,<sup>15</sup>N experiment was performed with the signal of the internal standard nitromethane in the subsequently measured <sup>1</sup>H,<sup>15</sup>N HMBC: For the recording of this gradient-enhanced HMBC spectra without decoupling with 512 *t*<sub>1</sub> increments, an acquisition time of 0.12 s, an interpulse delay of 1.5 s, and 16 or 24 repetitions per *t*<sub>1</sub> increment were necessary. Here, also a <sup>15</sup>N sweep rate of 550 ppm and resolution improvement via linear prediction were employed.

### <sup>19</sup>F NMR measurements

Conventional one-dimensional <sup>19</sup>F spectra with and without <sup>1</sup>H decoupling were measured with a sweep rate of 300 ppm and the acquisition of 128 k data points. Sixty-four repetitions were accumulated with an interpulse delay of 1.5 s.

### <sup>35</sup>Cl NMR measurements

Conventional one-dimensional <sup>35</sup>Cl spectra were measured with a sweep rate of 1500 ppm, acquisition of 8800 data points and an acquisition time of 100 ms. One thousand repetitions were accumulated with an interpulse delay of 100 ms.

### Mass spectrometry

Electrospray ionization mass spectra were recorded with a Bruker Esquire ~LC in the positive ion mode. Samples were applied via chromatographic separation on an RP 8 column with a 0.1% aqueous acetic acid/methanol gradient. The molecular ion was subjected to a second fragmentation step in the ion trap, delivering the fragment ions given in the supplementary experimental part.

## Results and Discussion

The results of the NMR experiments, especially the chemical shifts, are presented in tables for the different heteroaromatic nuclei (<sup>1</sup>H, <sup>13</sup>C, <sup>15</sup>N and <sup>35</sup>Cl; Tables 1 and 2); the complete listing of all chemical shifts are given in the supporting information section for each compound, together with the results of the mass spectroscopic analysis. The basic statistical evaluation of the chemical shifts is also given in the supporting information section with the results of the Shapiro–Wilk test for normal distribution, *F* or Levene's test for homogeneous variances, and student's *t* test, Welch's *t* test or the Mann–Whitney rank sum test for significant differences, depending on the results for normality and homoscedasticity testing.

### <sup>1</sup>H NMR data

The chemical shifts of the protons of the aroyl substituent are also given in the supporting information section and are not discussed any further; the substituent in position 3 of the pyridopyrimidinium moiety has no detectable influence on the chemical shifts of the aromatic protons of the heterocycle. The positive charge in the

heterocyclic skeleton is delocalized on positions 5, 6, 8 and 9a, leading to a high-frequency shift of the corresponding protons H-6 of about 1.2 ppm and H-8 of about 1 ppm, compared with H-7 and H-9, which resonate at 6.9 ppm (Table 1). We have shown before that the exchangeable proton is bound to N-1; there is no evidence for tautomeric isomers.<sup>[4]</sup> The signal of this NH proton is usually rather broad with line widths of several Hz up to 50 Hz (the broadening originating presumably on impurities like traces of excess of acid or water or exchange processes); in some cases, a triplet structure can be anticipated, in those cases the corresponding couplings of this NH proton can be observed in the <sup>1</sup>H,<sup>1</sup>H, <sup>1</sup>H,<sup>13</sup>C and <sup>1</sup>H,<sup>15</sup>N correlations as well. The aliphatic part of the heterocycle is forming a partially overlapping ABMN spin system, which was not investigated in detail; the chemical shifts of the corresponding protons could be sometimes only unraveled using the results of the <sup>1</sup>H,<sup>13</sup>C HSQC experiment.

The aromatic ring protons of the heterocycle show extensive coupling, typical coupling constants, which are found in the one-dimensional proton spectra of **4** in the range of 6.2–6.9 Hz [<sup>3</sup>*J*(H-6,H-7)], 6.8–7.0 Hz [<sup>3</sup>*J*(H-7,H-8)] and 8.4–8.9 Hz [<sup>3</sup>*J*(H-8,H-9)]. Additionally, long range couplings in the order of 1.0–1.5 Hz [<sup>4</sup>*J*(H-6,H-8)] and 0.5–1.2 Hz [<sup>4</sup>*J*(H-7,H-9)] are found. An unresolved <sup>5</sup>*J* coupling of H-6 with H-9 is observed in the H, H-COSY spectrum of **4**, too. For the methyl-substituted pyridopyrimidines **5**, **6** and **7**, the <sup>3</sup>*J* coupling constants were found to be in the same range. For structures **5**, **7** and **8**, the <sup>4</sup>*J* coupling constants were unresolved; for **6**, this <sup>4</sup>*J* coupling constant value was about 1.5–1.8 Hz.

The signal broadening of the aromatic protons of **5** to **8** is originated by a long range quartet splitting due to the methyl protons in the ring. For one derivative of **6**, this coupling constant could be determined to be 0.8 Hz. The corresponding H,H-COSY spectra do of course show all these long range couplings for the tetrahydropyridopyrimidines **5** to **8**. Also, crosspeaks for an interesting <sup>7</sup>*J* coupling of the methyl protons in position 8 of **6** and **8** with the aliphatic protons in position 4 can be found. The effect of the methyl group on the chemical shifts of the aromatic ring protons H-6 to H-9 is summarized in Table 3, where the average shifts of the hydroperchlorates of structures **4** to **8** are compared. The additivity of the methyl substitution effect in positions 6 and 8 (pyrimidines **5** and **6**) with the dimethyl derivatives **8** is also clearly visible (Table 3).

### <sup>13</sup>C NMR data

The focus of this discussion is on the aromatic carbon chemical shifts of the heterocyclic part of the substituted pyridopyrimidines **4–8**. The following pattern is recognizable for these carbon atoms, and the chemical shifts are summarized in Table 2. C-7 and C-9 resonate at low frequency of about 110–114 ppm and the partially positively charged carbon centers C-6 and C-8 at about 140 ppm; the annulated carbon atom C-9a is observed at 150 ppm. Introducing a methyl group in positions 6, 8 or 9 leads to a general high-frequency shift of about 10 ppm of the connected carbon center, a typical substituent shift for this group.<sup>[9]</sup> The additivity of the methyl substitution effect in positions 6 and 8 (pyrimidines **5** and **6**) on the <sup>13</sup>C chemical shifts compared with the dimethyl derivatives **8** is again clearly visible (Table 4).

For the unequivocal assignment, HSQC and HMBC spectra were recorded; for the pyridopyrimidines, a large number of CH long range couplings are observable, which are too numerous to be summarized in a single graphical representation. In general,

**Table 1.** Selected  $^1\text{H}$  NMR shifts for pyridopyrimidines **4–8**

Comp.	Anion	H-6	6-Me	H-7	H-8	8-Me	H-9	9-Me	NH
<b>4a</b>	$\text{ClO}_4^-$	8.03		6.87	7.83		6.99		9.05
<b>4b</b>	$\text{ClO}_4^-$	8.01		6.86	7.78		6.99		9.35
<b>4e</b>	$\text{ClO}_4^-$	8.01		6.86	7.79		7.00		9.40
<b>4f</b>	$\text{ClO}_4^-$	8.02		6.85	7.80		7.05		9.61
<b>4c</b>	$\text{Cl}^-$	8.00		6.86	7.81		6.99		9.35
<b>4d</b>	$\text{Cl}^-$	8.01		6.84	7.79		7.16		10.00
<b>4g</b>	$\text{Cl}^-$	8.06		6.84	7.78		7.19		10.18
<b>5a</b>	$\text{ClO}_4^-$		2.51	6.81	7.70		6.87		9.29
<b>5b</b>	$\text{ClO}_4^-$		2.52	6.81	7.70		6.87		9.30
<b>5c</b>	$\text{ClO}_4^-$		2.51	6.80	7.69		6.86		9.28
<b>5e</b>	$\text{ClO}_4^-$		2.53	6.83	7.72		6.90		9.36
<b>5d</b>	$\text{Cl}^-$		2.53	6.81	7.70		6.97		9.66
<b>6a</b>	$\text{ClO}_4^-$	7.92		6.72		2.30	6.82		9.44
<b>6b</b>	$\text{ClO}_4^-$	7.91		6.73		2.31	6.78		9.28
<b>6c</b>	$\text{ClO}_4^-$	7.93		6.76		2.33	6.79		9.22
<b>6d</b>	$\text{ClO}_4^-$	7.93		6.75		2.33	6.78		9.20
<b>6e</b>	$\text{ClO}_4^-$	7.92		6.74		2.32	6.77		9.28
<b>6f</b>	$\text{ClO}_4^-$	7.91		6.73		2.31	6.80		9.35
<b>6g</b>	$\text{ClO}_4^-$	7.90		6.73		2.32	6.76		9.14
<b>6i</b>	$\text{ClO}_4^-$	7.93		6.74		2.32	6.77		9.13
<b>6k</b>	$\text{ClO}_4^-$	7.91		6.73		2.32	6.75		9.16
<b>6m</b>	$\text{ClO}_4^-$	7.91		6.73		2.31	6.81		9.38
<b>6n</b>	$\text{ClO}_4^-$	7.90		6.73		2.32	6.76		9.19
<b>6o</b>	$\text{ClO}_4^-$	7.91		6.73		2.32	6.76		9.17
<b>6h</b>	$\text{Cl}^-$	7.98		6.71		2.30	6.95		10.00
<b>6l</b>	$\text{Cl}^-$	7.94		6.72		2.30	6.91		9.88
<b>6p</b>	$\text{Cl}^-$	7.92		6.70		2.30	6.90		9.83
<b>7a</b>	$\text{ClO}_4^-$	7.97		6.86	7.73			2.17	8.54
<b>7b</b>	$\text{ClO}_4^-$	7.95		6.85	7.72			2.17	8.55
<b>7c</b>	$\text{ClO}_4^-$	7.95		6.85	7.73			2.18	8.56
<b>8a</b>	$\text{ClO}_4^-$		2.50	6.71		2.28	6.68		9.21
<b>8b</b>	$\text{ClO}_4^-$		2.49	6.71		2.28	6.66		9.13
<b>8c</b>	$\text{ClO}_4^-$		2.48	6.71		2.28	6.67		9.14
<b>8d</b>	$\text{Cl}^-$		2.48	6.80		2.26	6.69		9.71

the aliphatic protons of the heterocycle show crosspeaks with the other aliphatic carbon atoms and the carbon atom of the carbonyl group, which resonates at around 196 ppm. H-2 couples with C-9a and H-4 with C-6. For the pyridopyrimidines **4–8**, which have a suitably resolved triplet signal for the NH proton in position 1, CH long range couplings to C-9 and C-9a are found.

For the pyridopyrimidinium salts **4**, the following couplings are observed for the aromatic moiety part of the heterocycle: H-6 couples with C-4, C-7, C-8, C-9 (w, weak) and C-9a; H-7 couples with C-6, C-9 and C-9a (w); H-8 couples with C-6, C-9 (w) and C-9a; and finally, H-9 couples with C-4 (w), C-6 (w), C-7, C-8 (w) and C-9a. The assignment of a crosspeak as a weak signal is based on the investigation of the one-dimensional projection of the column of the respective proton in the two-dimensional spectrum; here, signals with less than about 10% of the intensity of the major peaks are denominated weak. Reference values for the unsubstituted pyridinium ion as model compound are reported by Kalinowski *et al.*<sup>[10]</sup>; they give the following coupling constants: 3.3 Hz for  $^2J(\text{H-3}, \text{C-2})$  and 5.1 Hz for  $^2J(\text{H-2}, \text{C-3})$ .<sup>[10a]</sup> Couplings over three bonds are in the range of 6.1 to 7.2 Hz.<sup>[10b]</sup> Couplings over four bonds in the unprotonated

pyridine are reported to be  $-0.9$  Hz for H-5 with C-2 and  $-1.7$  Hz for H-6 with C-3.<sup>[10c]</sup> In order to substantiate the discussion on diagnostic CH long range couplings, the following values were determined for **4a** using the EXSIDE pulse program,<sup>[11]</sup> a two-dimensional technique, starting with a selective pulse on one proton and determining the coupling constant by the splitting of the carbon resonances in the indirect dimension. This technique uses indirect detection via a double INEPT transfer with gradient enhancement<sup>[11]</sup> and allows the usage of the samples already analyzed. Recently, the usage of a proton and carbon selective version (Selexside) was published.<sup>[12]</sup> Thus, the following values were obtained for **4a**: H-6 couples with C-4 (4.1 Hz), C-7 (3.2 Hz), C-9 (ca. 1 Hz) and C-9a (7.2 Hz); H-7 couples with C-6 (6.3 Hz), C-8 ( $<2$  Hz), C-9 (7.9 Hz) and C-9a ( $<2$  Hz); and H-8 couples with C-6 (9.4 Hz), C-7 ( $<2$  Hz), C-9 (0.9 Hz) and C-9a (9.1 Hz). Finally, H-9 shows CH long range couplings to C-4 ( $<2$  Hz), C-6 ( $<2$  Hz), C-7 (7.4 Hz), C-8 ( $<2$  Hz) and C-9a (3.1 Hz).

In the 6-methyl-substituted derivatives **5**, crosspeaks of the protons of the methyl group with C-4 (w), C-6 and C-7 are observed. H-7 couples with C-6, 6-Me and C-9. H-8 couples also with C-6, C-7 (w), C-9 and C-9a. H-9 shows coupling to C-4 (w), C-6 (w), C-7, C-8 (w) and C-9a.

Table 2. Selected  $^{13}\text{C}$ ,  $^{15}\text{N}$  and  $^{35}\text{Cl}$  NMR shifts for pyridopyrimidines 4–8

Comp.	Anion	N-1	C-2	C-3	C-4	N-5	C-6	6-Me	C-7	C-8	8-Me	C-9	9-Me	C-9a	Cl
4a	$\text{ClO}_4^-$	-291.2	40.3	35.2	51.0	-225.2	139.5		112.1	141.2		114.4		151.0	1013
4b	$\text{ClO}_4^-$	n.d.	40.3	35.1	51.1	-225.3	139.4		112.0	141.2		114.4		151.0	1013
4e	$\text{ClO}_4^-$	-291.0	40.7	34.6	51.3	-225.0	139.5		112.0	141.1		114.4		151.0	1011
4f	$\text{ClO}_4^-$	-290.9	40.2	35.2	51.0	-225.6	139.4		111.8	141.1		114.4		151.0	1011
4c	$\text{Cl}^-$	n.d.	40.2	35.3	50.9	-225.5	139.5		112.1	141.1		114.4		151.0	-
4d	$\text{Cl}^-$	-289.4	39.9	35.4	50.8	-226.2	139.4		111.9	140.9		114.4		151.0	-
4g	$\text{Cl}^-$	-288.4	40.4	34.8	51.0	-225.9	139.3		111.8	140.8		114.4		151.1	-
5a	$\text{ClO}_4^-$	-291.6	40.2	35.6	46.6	-222.1	148.1	19.4	112.9	140.5		112.1		152.0	1013
5b	$\text{ClO}_4^-$	-291.4	40.5	35.1	47.0	-222.2	148.1	19.4	112.9	140.5		112.2		152.0	1013
5c	$\text{ClO}_4^-$	n.d.	40.3	35.8	46.8	-222.3	148.2	19.5	113.1	140.7		112.3		152.0	1011
5e	$\text{ClO}_4^-$	-290.9	40.5	35.6	47.0	-222.0	148.2	19.4	112.9	140.6		112.2		152.0	1011
5d	$\text{Cl}^-$	-290.3	40.2	35.7	46.7	-222.4	148.1	19.5	112.8	140.4		112.2		152.0	-
6a	$\text{ClO}_4^-$	-293.3	40.3	35.5	50.5	-229.3	138.6		114.2	153.1	20.9	112.6		150.6	1011
6b	$\text{ClO}_4^-$	-293.7	40.1	35.5	50.4	-229.2	138.6		114.2	153.2	20.9	112.6		150.5	1011
6c	$\text{ClO}_4^-$	-293.7	40.5	35.4	50.8	-228.9	138.7		114.2	153.3	20.9	112.6		150.6	1013
6d	$\text{ClO}_4^-$	-293.7	40.5	35.3	50.8	-228.8	138.7		114.2	153.2	20.9	112.6		150.6	1011
6e	$\text{ClO}_4^-$	-294.1	40.3	35.5	50.6	-229.2	138.7		114.3	153.3	20.9	112.6		150.6	1011
6f	$\text{ClO}_4^-$	-293.5	40.1	35.5	50.5	-229.3	138.6		114.2	153.2	20.9	112.5		150.6	1011
6g	$\text{ClO}_4^-$	-294.0	40.3	35.1	50.7	-229.0	138.6		114.2	153.2	20.9	112.6		150.5	1011
6i	$\text{ClO}_4^-$	-294.0	40.3	35.4	50.6	-229.0	138.7		114.2	153.2	20.9	112.6		150.6	1011
6k	$\text{ClO}_4^-$	-293.8	40.3	35.2	50.6	-229.0	138.7		114.2	153.2	20.9	112.5		150.5	1011
6m	$\text{ClO}_4^-$	-293.5	39.8	35.5	50.3	-229.5	138.6		114.3	153.2	20.9	112.6		150.5	1011
6n	$\text{ClO}_4^-$	-293.6	40.4	35.0	50.7	-228.8	138.6		114.2	153.2	20.9	112.5		150.5	1011
6o	$\text{ClO}_4^-$	-293.8	40.4	35.0	50.7	-228.9	138.7		114.2	153.2	20.9	112.5		150.5	1011
6h	$\text{Cl}^-$	-291.4	40.1	35.5	50.4	-229.4	138.6		114.0	152.7	20.9	112.5		150.6	-
6l	$\text{Cl}^-$	-291.9	39.9	35.9	50.3	-229.9	138.6		114.1	152.9	20.9	112.5		150.6	-
6p	$\text{Cl}^-$	-291.6	40.3	35.0	50.6	-229.3	138.6		114.0	152.8	20.9	112.5		150.6	-
7a	$\text{ClO}_4^-$	-292.4	41.2	35.3	51.5	-225.2	137.4		111.8	140.1		123.0	16.5	150.1	1011
7b	$\text{ClO}_4^-$	-292.5	41.3	35.2	51.6	-225.1	137.4		111.8	140.1		123.0	16.5	150.1	1013
7c	$\text{ClO}_4^-$	-292.8	41.6	34.7	51.8	-224.9	137.4		111.8	140.1		123.0	16.5	150.1	1011
8a	$\text{ClO}_4^-$	-293.6	40.4	36.0	46.4	-226.1	147.2	19.2	115.1	152.3	20.7	110.6		151.6	1011
8b	$\text{ClO}_4^-$	-293.5	40.2	35.9	46.4	-225.8	147.6	19.2	115.1	152.4	20.7	110.6		151.5	1011
8c	$\text{ClO}_4^-$	-293.5	40.4	35.9	46.6	-225.8	147.2	19.2	115.1	152.4	20.7	110.6		151.6	1011
8d	$\text{Cl}^-$	-291.5	40.2	35.7	46.6	-226.1	147.1	19.2	114.9	152.0	20.7	110.6		151.6	-

**Table 3.** Summary of average  $^1\text{H}$  NMR chemical shifts for the different substitution pattern in **4** to **8**

Comp.	H-6/6-Me	H-7	H-8/8-Me	H-9/9-Me	NH
<b>4</b> ( $n=4$ )	8.02	6.86	7.80	7.01	9.35
<b>5</b> ( $n=4$ )	2.52	6.81	7.70	6.88	9.31
$\Delta$		-0.05	-0.10	-0.13	-0.04
<b>6</b> ( $n=12$ )	7.92	6.74	2.32	6.78	9.24
$\Delta$	-0.10	-0.12		-0.23	-0.11
<b>7</b> ( $n=3$ )	7.96	6.85	7.73	2.17	8.55
$\Delta$	-0.03	-0.01	-0.07		-0.80
<b>8</b> ( $n=3$ )	2.49	6.72	2.28	6.68	9.16
$\Delta$		-0.14		-0.33	-0.19
$\Delta_{\text{calculated}}$		-0.17		-0.36	-0.15

Only the perchlorates were compared;  $\Delta$  is the difference in chemical shift to the unsubstituted pyrimidine **4**; and  $\Delta_{\text{calculated}}$  is the calculated difference for substituted pyrimidines **8** using the incremental shift values of **5** and **6**.

In the same way, the crosspeaks of pyridopyrimidines **6** in the HMBC spectra are given: H-6 couples with C-4, C-7, C-8 and C-9a; H-7 couples with C-6, 8-Me, C-9 and C-9a (*w*); the protons of the methyl group in position 8 couple with C-7, C-8 and C-9; and finally, H-9 shows couplings with C-4 (*w*), C-7, 8-Me and C-9a. Exemplarily for **6o**, the following values for the coupling constants were determined: H-6 with C-4 (4.1 Hz), C-7 (2.8 Hz), C-8 (ca. 8 Hz), C-9 (<2 Hz) and C-9a (7.3 Hz); H-7 with C-6 (5.7 Hz), C-8 (<2 Hz), 8-Me (3.5 Hz), C-9 (6.8 Hz) and C-9a (<2 Hz); and H-9 with C-4 (<2 Hz), C-6 (<2 Hz), C-7 (7.9 Hz), C-8 (<2 Hz), 8-Me (4.9 Hz) and C-9a (2.3 Hz). The protons of the methyl group couple with C-7 (4.7 Hz), C-8 (6.5 Hz) and C-9 (approx. 5 Hz).

For the pyridopyrimidinium salts **7**, the following CH long range couplings are observed in general: H-6 couples with C-4, C-7, C-8, C-9 (*w*) and C-9a; H-7 with C-6, C-9 and C-9a (*w*); and H-8 with C-6, 9-Me and C-9a. The protons of the methyl group couple with C-6 (*w*), C-7 (*w*), C-8, C-9 and C-9a. For **7c**, the following values for the CH long range coupling constants were determined: H-6 with C-4 (3.6 Hz), C-7 (3.1 Hz), C-8 (8.6 Hz), C-9 (0.7 Hz) and C-9a (7.2 Hz); H-7 with C-6 (5.6 Hz), C-8 (<2 Hz), C-9 (7.7 Hz) and C-9a (<2 Hz); and H-8 with C-6 (8.0 Hz), C-7 (<2 Hz), C-9 (<2 Hz), 9-Me (5.3 Hz) and C-9a (9.3 Hz). The protons of the methyl group in position 9 show the following couplings to C-6 (<2 Hz), C-8 (5.5 Hz), C-9 (6.7 Hz) and C-9a (4.2 Hz).

Eventually, the CH long range couplings of the pyridopyrimidines **8** bearing two methyl groups are analyzed. The protons of the methyl group in position 6 couple with C-4, C-6, C-7 and C-9 (*w*), and H-7 couples with C-6, 6-Me, 8-Me and C-9; the protons of the methyl group in position 8 exhibit couplings to C-7, C-8 and C-9, and H-9 couples to C-7, 8-Me and C-9a. For one example, **8c**, the following coupling constants were determined: The protons of the methyl group in position 6 couple to C-4 (<2 Hz), C-6 (6.8 Hz), C-7 (4.7 Hz), C-8 (<2 Hz) and C-9 (<2 Hz), and H-7 couples to C-6 (5.1 Hz), 6-Me (3.7 Hz), C-8 (<2 Hz), 8-Me (4.4 Hz), C-9 (5.0 Hz) and C-9a (<2 Hz); the protons of the methyl group in position 8 couple to C-7 (6.6 Hz), C-8 (4.6 Hz) and C-9 (5.7 Hz), and H-9 couples to C-6 (<2 Hz), C-7 (6.9 Hz), C-8 (<2 Hz) and C-9a (3.5 Hz).

So, the heterocyclic framework shows many diagnostic CH long range couplings, besides the usually large coupling constants over three bonds; the large coupling constants over two bonds in the vicinity of the positively charged heteroatom have to be considered for this class of compounds as well.

### $^{15}\text{N}$ NMR data

$^{15}\text{N}$  NMR spectroscopy has developed to a routinely employed technique in structure elucidation and analysis,<sup>[13]</sup> for example in natural products,<sup>[14]</sup> and in the investigation of drugs and drug decomposition products<sup>[15]</sup> despite its inherent low sensitivity that is overcome by indirect proton detection. So, all 34 compounds were investigated by proton-detected HSQC and HMBC experiments; the chemical shifts were evaluated by the resolution-enhanced two-dimensional data sets, whereby nitromethane was employed as internal standard (Fig. 2). For nearly all structures, two signals are observed in the range of -220 to -228 ppm and -290 to -294 ppm, corresponding to the charged pyridinium nitrogen atom and the amino function (Tables 2 and 4). Here, also the comparison with literature data is helpful. Städeli *et al.* reported chemical shifts of the protonated 2-aminopyridine of -229.5 and -292.6 ppm in fluorosulfonic acid and -226.0/-305.6 ppm in trifluoroacetic acid relative to neat external nitromethane.<sup>[16]</sup> These values can be referenced by subtraction of 2 ppm to values relative to nitromethane in DMSO.<sup>[17]</sup> More recently, Beltrame *et al.* investigated the protonation of monoaminopyridines, and they reported values relative to deuterated *N,N*-DMF,<sup>[18]</sup> which requires re-referencing. For *N,N*-DMF-*d*<sub>7</sub>, LeGoff reported a chemical shift of 105 ppm at

**Table 4.** Summary of average  $^{13}\text{C}$  and  $^{15}\text{N}$  NMR chemical shifts for the different substitution pattern in **4** to **8**

	N-1	C-2	C-3	C-4	N-5	C-6	6-Me	C-7	C-8	8-Me	C-9	9-Me	C-9a
<b>4</b>	-291.0	40.4	35.0	51.1	-225.3	139.5		112.0	141.2		114.4		151.0
<b>5</b>	-291.3	40.4	35.5	46.9	-222.2	148.2	19.4	113.0	140.6		112.2		152.0
$\Delta$	-0.3	0.0	0.5	-4.2	+3.1	8.7		1.0	-0.6		-2.2		1.0
<b>6</b>	-293.7	40.3	35.3	50.6	-229.1	138.7		114.2	153.2	20.9	112.6		150.6
$\Delta$	-2.7	-0.1	0.3	-0.5	-3.8	-0.8		2.2	12.0		-1.8		-0.4
<b>7</b>	-292.6	41.4	35.1	51.6	-225.1	137.4		111.8	140.1		123.0	16.5	150.1
$\Delta$	-1.6	1.0	0.1	0.5	0.2	-2.1		-0.2	-1.1		8.6		-0.9
<b>8</b>	-293.5	40.3	35.9	46.5	-225.9	147.3	19.2	115.1	152.4	20.7	110.6		151.6
$\Delta$	-2.5	-0.1	0.9	-4.6	-0.6	7.8		3.1	11.2		-3.8		0.6
$\Delta_{\text{calculated}}$	-3.0	-0.1	0.8	-4.7	-0.7	7.9		3.2	11.4		-4.0		0.6

Only the perchlorates were compared;  $\Delta$  is the difference in chemical shift to the unsubstituted pyrimidine **4**; and  $\Delta_{\text{calculated}}$  is the calculated difference for substituted pyrimidines **8** using the incremental shift values of **5** and **6**.

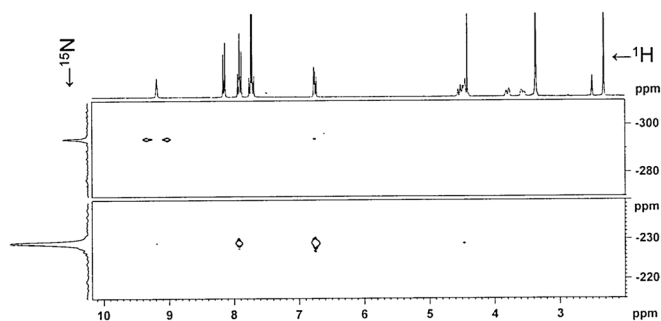


**Figure 2.**  $^1\text{H}, ^{15}\text{N}$  HMBC spectrum of the most potent NOS inhibitor in the series<sup>[6]</sup> **6e** in  $\text{DMSO}-d_6$ .

353 K,<sup>[19]</sup> and Kohlemainen gave a shift for *N,N*-DMF of 103.8 ppm<sup>[20]</sup> (obviously, both values are referenced to the ammonia scale); these values can be recalculated to values relative to nitromethane in  $\text{DMSO}$ <sup>[17]</sup> affording a chemical shift of DMF versus nitromethane of  $-277.2$  and  $-278.4$  ppm, respectively. We measured a value of  $-276.6$  ppm for the chemical shift of undeuterated *N,N*-DMF versus internal nitromethane in  $\text{DMSO}-d_6$ , which is in accordance with the above reported values. So, the shifts of Beltrame reported for a protonated 2-aminopyridine in  $\text{CDCl}_3/\text{DMSO}-d_6$  7/3 are calculated to be  $-228.1$  and  $-302.5$  ppm. Therefore, the description of the pyrido[1,2-*a*]pyridines as derivatives of alkylated aminopyridinium ions is confirmed also by the chemical shifts of the  $^{15}\text{N}$  nuclei, as Bertrame *et al.* proved the protonation of the pyridine nitrogen in their investigation.

The effect of methyl group substitution on the chemical shift of the partially positively charged nitrogen atom N-5 can be summarized as +3, approx. 0 and  $-4$  ppm for the methyl group in *ortho*, *meta* and *para* positions, of the nitrogen, corresponding to the pyridopyrimidines **5**, **7** and **6**, when compared with structures **4** (Table 4). For uncharged pyridine and quinoline, this methyl group substituent effect has been reported to be in the order of +4.9, 0, +8.3 ppm and +4.9, +0.2, +5.3 ppm, respectively.<sup>[21]</sup> So, the shielding effect of the additional methyl group in *ortho* position and the negligible effect in *meta* position is also observed for the pyridopyrimidines **4–8**; however, the interesting deshielding of the methyl group *para* to the nitrogen might require a more theoretical analysis. The effect of the methyl group substitution on the chemical shift of the amine function is of course much smaller; in all cases, methyl group substitution leads to a more or less pronounced deshielding ( $-0.3$  to  $-2.7$  ppm).

For nearly all structures, the  $^1J$  coupling constant for H with N-1 was determined from the HMBC spectrum as a rough estimate in the range of 92 to 95 Hz, proving the strong involvement of the nitrogen lone pair in mesomeric stabilization of the positive charge.

The observed diagnostic NH long range couplings are summarized in graphical form; as in the case of CH long range correlations, only sufficiently narrow signals for the NH proton led to observable correlations in the H,N HMBC spectra (Fig. 3).

### $^{35}\text{Cl}$ NMR data

The chlorine nucleus is usually of no importance in structure elucidation; because of the quadrupole moment, it exhibits broad lines, which are of no value in the investigation of organic structures. Also, as a counterion for organic salts like the pyrimidinium ions in  $\text{DMSO}-d_6$ , the surrounding of the nucleus is not symmetric, leading to broad lines, which are difficult or

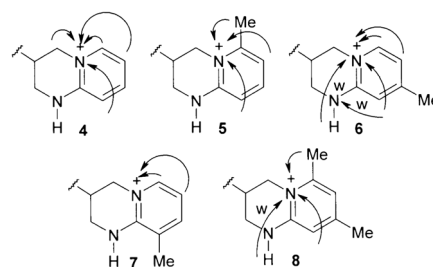


**Figure 3.** Graphical representation of diagnostic NH long range couplings in pyridopyrimidines **4–8** (w, weak).

impossible to detect. Only as a perchlorate, the chlorine resonance can be detected easily even in organic solvents; so, the measurement of this signal at about +1010 ppm relative to the chlorine in sodium chloride in water was employed to proof the identity of the perchlorate anion. This perchlorate signal is of course not influenced by the type of compound and the substitution position of the methyl group (Table 2).

### Influence of the counter ion

The comparison of chemical shifts of pyrimidinium perchlorates versus chlorides requires some statistical calculations. All results are summarized in the supporting information section in tables 1–10. For these calculations, the rounded numbers in tables 1 and 2 are used; chemical shift differences that are below 0.02 ( $^1\text{H}$ ), 0.1 ( $^{13}\text{C}$ ) and 0.4 ppm ( $^{15}\text{N}$ ) are considered to be near the experimental error (especially for the  $^{15}\text{N}$  NMR results, which are extracted from two-dimensional spectra). For the pyridopyrimidines **4–8**, the relevant and significant differences in  $^1\text{H}$ ,  $^{13}\text{C}$  and  $^{15}\text{N}$  NMR shifts that are observed are summarized in Table 5.

A diagnostic difference can be observed in general for NH, H-9, N-1 and C-8; the difference is smaller and not uniformly observed for all pyridopyrimidines for N-5 and other proton and carbon shifts. It can be speculated that the NH function is more involved in any ion pairing process in solution; this might explain the strong effects on chemical shifts on this part of the molecule, especially a  $\Delta\delta$  value of about 0.4 ppm for NH and a  $\Delta\delta$  of 0.1 ppm for H-9 are observed. The group of Burgess *et al.* investigated  $^1\text{H}$  and  $^{15}\text{N}$  NMR chemical shift changes upon salt formation for simple bases like pyridine and reported greater chemical shift changes with stronger acids<sup>[22]</sup>; however, perchloric acid can be considered as the stronger acid, also in  $\text{DMSO}$ ; so, a greater shift compared with the unprotonated base should be observed for the perchlorate. Similarly, Somoshekar *et al.*<sup>[23]</sup> reported on the influence of the counter ion (maleate, mesylate and chloride) for trimipramine hydrochloride in  $\text{CDCl}_3$  and derived a linear correlation between  $pK_a$  value and chemical shift difference compared with the nonprotonated base for  $^{15}\text{N}$  in the range of  $\Delta\delta = 0.5$  ppm per  $pK_a$  unit.<sup>[23]</sup> When taking a  $pK_a$  value for  $-7$  for hydrochloric acid and  $-10$  for perchloric acid, a difference for the  $^{15}\text{N}$  resonance of N-1 in the range of 1.5 ppm would be expected, but in this case, the chlorides show the greater shift difference (calculating a chemical shift by referencing to nitromethane in  $\text{DMSO}$  of about  $-315.6$  ppm for nonprotonated aminopyridine<sup>[18]</sup>). Recently, Metaxas and Cohrt reported on interesting counter ion effect in strychnine salts effecting  $^1\text{H}$  and  $^{13}\text{C}$  shifts in  $\text{CDCl}_3$  and  $\text{CD}_3\text{OD}$ , but not in  $\text{D}_2\text{O}$ .<sup>[24]</sup> Vinalryay and Pandiarajan discussed solvent-free and

**Table 5.** Relevant and significant chemical shift differences for pyridopyrimidines **4–6** and **8** between perchlorates and chlorides,  $p < 0.05$ , if not stated otherwise

Comp.	Atom (chemical shift difference $\Delta\delta$ in ppm)
<b>4</b>	NH ( $\Delta\delta = 0.44$ , $p = 0.11$ ), H-9 ( $\Delta\delta = 0.10$ , $p = 0.11$ ), N-1 ( $\Delta\delta = 1.3$ , $p = 0.14$ ), N-5 ( $\Delta\delta = 0.6$ ), C-8 ( $\Delta\delta = 0.2$ )
<b>5</b>	NH ( $\Delta\delta = 0.35$ ), H-9 ( $\Delta\delta = 0.10$ ), N-1 ( $\Delta\delta = 1.0$ ), N-5 ( $\Delta\delta = 0.3$ ), C-8 ( $\Delta\delta = 0.2$ )
<b>6</b>	NH ( $\Delta\delta = 0.66$ ), N-1 ( $\Delta\delta = 2.1$ ), N-5 ( $\Delta\delta = 0.5$ ), C-7 ( $\Delta\delta = 0.2$ ), C-8 ( $\Delta\delta = 0.4$ )
<b>8</b>	NH ( $\Delta\delta = 0.55$ ), H-7 ( $\Delta\delta = 0.09$ ), H-9 ( $\Delta\delta = 0.02$ , $p = 0.074$ ), N-1 ( $\Delta\delta = 2.0$ ), C-3 ( $\Delta\delta = 0.2$ ), C-8 ( $\Delta\delta = 0.4$ )

solvent containing ion pairing for picrates, nitrates and chlorides of protonated substituted piperidinium ions in different solvents.<sup>[25]</sup>

On the other hand, Barczynski reported small counter ion effects of <sup>1</sup>H and <sup>13</sup>C nuclei within experimental errors of complexes of various acids with 1-methylquinolinium-3-carboxylate, a zwitter ion.<sup>[26]</sup>

So, to date, there is no general predictability of the influence of the counter ion in different solvents and depending on the acid strength of the conjugate anion. However, the chemical shift differences of the pyridopyrimidines **4–8** investigated here, at least for some nuclei, are sufficiently large to allow the indirect detection of the type of counter ion, namely either the chloride or perchlorate anion.

### Mass spectrometry

For the assignment and proof of structure, mass spectra after electrospray ionization in the positive ionization mode were measured, and the base peak, which was the protonated molecular ion, was fragmented in a second step (MS/MS) in the ion trap. This way, the information about the number of methyl groups of the pyrido[1,2-*a*]pyrimidine skeleton was confirmed, but the position of the methyl group could not be determined. For the smaller pyridopyrimidines, the defragmentation of the protonated pyrimidine can be explained via a simple retro Diels–Alder reaction, delivering the uncharged enone together with an *o*-chinoid heterocyclic structure bearing none, one or two methyl substituents.

### Conclusion

A series of 1,2,3,4-tetrahydro-pyrido[1,2-*a*]pyrimidinium perchlorates and chlorides, with and without methyl substituents in the unsaturated part of the heterocycle, were analyzed, affording a robust data set of <sup>1</sup>H, <sup>13</sup>C, <sup>15</sup>N and <sup>35</sup>Cl chemical shifts in DMSO-*d*<sub>6</sub>. <sup>1</sup>H, <sup>13</sup>C and <sup>1</sup>H, <sup>15</sup>N long range couplings were investigated, which are an important tool in structure elucidation. Exemplarily, for a few compounds, the CH long range coupling constants were determined using the exsided pulse program. Significant differences for the <sup>15</sup>N chemical shifts of N-5 were found, depending on the position of the methyl substituent. Large and significant shift differences were found for all the nuclei under investigation when comparing perchlorates with chlorides; here, especially at the NH signal, N-1, C-8 and H-9 have

to be mentioned. The perchlorate anion could be determined directly by measurement of the <sup>35</sup>Cl resonance.

### References

- [1] U. Girreser, D. Heber, M. Schütt. *Synthesis* **1998**, 30, 715–717.
- [2] U. Girreser, D. Heber. *J. Prakt. Chem.* **2000**, 342, 230–234.
- [3] U. Girreser, D. Heber, M. Schütt. *Synthesis* **1999**, 31, 1637–1641.
- [4] U. Girreser, D. Heber, M. Schütt. *Synlett* **1998**, 9, 263–264.
- [5] U. Bluhm, J.-L. Boucher, B. Clement, U. Girreser, D. Heber, B. Ramassamy, U. Wolschendorf. *J. Het. Chem.* in press.
- [6] U. Bluhm, J.-L. Boucher, U. Buss, B. Clement, F. Friedrich, U. Girreser, D. Heber, T. Lam, M. Lepoivre, M. Rostaie-Gerylow, U. Wolschendorf. *Eur. J. Med. Chem.* **2009**, 44, 2877–2887.
- [7] R. Paira, A. Maity, S. Mondal, S. Naskar, K. B. Sahu, P. Saha, A. Hazra, E. Padmanaban, S. Bannerjee, N. B. Mondal. *Tetrahedron Lett.* **2011**, 52, 1653–1657.
- [8] M. Findeisen, T. Brand, S. Berger. *Magn. Reson. Chem.* **2007**, 45, 175–178.
- [9] E. Pretsch, P. Bühlmann, C. Affolter, M. Badertscher, *Spektroskopische Daten zur Strukturaufklärung organischer Verbindungen*, 4th edn, Springer, Berlin, **2001**.
- [10] H.-O. Kalinowski, S. Berger, S. Braun, <sup>13</sup>C-NMR-Spektroskopie, Thieme, Stuttgart, **1984**; a) p. 472, b) p. 489, c) p. 491.
- [11] V. V. Krishnamurthy. *J. Magn. Res. Ser. A* **1996**, 121, 33–41.
- [12] C. P. Butts, B. Heise, G. Tatolo. *Org. Lett.* **2012**, 14, 3256–3259.
- [13] R. Marek, A. Lyčka. *Curr. Org. Chem.* **2002**, 6, 35–66.
- [14] G. E. Martin, M. Solntseva, A. J. Williams. <sup>15</sup>N NMR spectroscopy, in *Modern Alkaloids*, (Ed: E. Fattorusso, O. Tagliatalate-Scafati), Wiley-VCH, Weinheim, **2008**, pp. 409–471.
- [15] A. Czyski, U. Girreser, T. Hermann. *J. Mol. Struct.* **2013**, 1036, 111–114.
- [16] W. Städeli, W. von Philipsborn, A. Wick, I. Kompš. *Helv. Chim. Acta* **1980**, 63, 504–522.
- [17] R. M. Claramunt, D. Sanz, C. Lopéz, J. A. Jiménez, M. L. Jimeno, J. Elguero, A. Fruchier. *Magn. Res. Chem.* **1997**, 35, 35–75.
- [18] P. Beltrame, E. Cadoni, C. Floris, G. Gelli, A. Lai. *Spectrochim. Acta A* **2002**, 25, 2639–2697.
- [19] G. Le Goff, M. T. Martin, C. Servy, S. Cortial, P. Lopes, A. Bialecki, J. Smadja, J. Ouazzani. *J. Nat. Prod.* **2012**, 75, 915–919.
- [20] E. Kolehmainen, *Novel Applications of Dynamic NMR in Organic Chemistry*, in *Annual Reports on NMR Spectroscopy*, vol 49, (Ed: G. Webb), Academic Press, U.K., **2003**, pp. 2–41.
- [21] L. Stefaniak, J. D. Roberts, M. Witanowski, G. A. Webb. *Org. Magn. Res.* **1984**, 22, 201–208.
- [22] H. Kim, J. Gao, D. J. Burgess. *Int. J. Pharm.* **2009**, 377, 105–111.
- [23] B. S. Somashekar, G. A. Nagana Gowda, A. R. Ramesha, C. L. Khetrapal. *Magn. Res. Chem.* **2005**, 43, 166–170.
- [24] A. E. Metaxas, J. R. Cort. *Magn. Res. Chem.* **2013**, 51, 292–298.
- [25] V. Vimalraj, K. Pandiarajan. *Magn. Res. Chem.* **2011**, 49, 682–687.
- [26] P. Barczynski, M. Szafran. *Polish J. Chem.* **2009**, 83, 1061–1074.